Modulation of Recombinant Human Prostate-Specific Antigen: Activation by Hofmeister Salts and Inhibition by Azapeptides†

Xinyi Huang,‡,§ Christopher T. Knoell,‡ Gary Frey,‖,⊥ Maryam Hazegh-Azam,@,# Armen H. Tashjian, Jr.,○ Lizbeth Hedstrom,*,@ and Robert H. Abeles,@,+

Department of Biochemistry and Programs in Biochemistry and Bioorganic Chemistry, Brandeis University, Waltham, Massachusetts 02454, and Department of Cancer Cell Biology, Harvard School of Public Health, 665 Huntington Avenue, Boston, Massachusetts 02115

Appendix: Thermodynamic Interpretation of the Activation by Concentrated Salts

Serge N. Timasheff‡

Department of Biochemistry, Brandeis University, Waltham, Massachusetts 02454

Received February 21, 2001; Revised Manuscript Received July 5, 2001

ABSTRACT: Prostate specific antigen (PSA, also known as human kallikrein 3) is an important diagnostic indicator of prostatic disease. PSA exhibits low protease activity ($>10^4$-fold less than chymotrypsin) under the usual in vitro assay conditions. In addition, PSA does not react readily with prototypical serine protease inactivators. We expressed human PSA (rh-PSA) in *Escherichia coli* and have demonstrated that rh-PSA has properties similar to those of native PSA isolated from human seminal fluid. Both PSA and rh-PSA are $>10^3$-fold more active in the presence of 1.3 M Na_2SO_4. This activation is anion-dependent, following the Hofmeister series when normality is considered: $SO_4^{2-} \approx$ citrate $>$ Ac^- $>$ Cl^- $>$ Br^- $>$ I^-. The nature of the cation has little effect on salt activation. The rate of inactivation of rh-PSA by DFP is 30-fold faster in the presence of 0.9 M Na_2SO_4, and the rate of inactivation by Suc-Ala-Ala-Pro-Phe-CK is >20-fold faster under these conditions. Azapeptides containing Phe or Tyr at position P_1 also inactivate rh-PSA in the presence of high salt concentrations. These compounds represent the first described inhibitors designed to utilize the substrate binding subsites of PSA. CD spectroscopy demonstrates that the conformation of rh-PSA changes in the presence of high salt concentrations. Analytical ultracentifugation and dynamic light scattering indicate that PSA remains monomeric under high-salt conditions. Interestingly, human prostatic fluid contains as much as 150 μmol citrate/g wet weight, which suggests that salt concentrations may regulate PSA activity in vivo.

Prostate specific antigen (PSA)[1] is a member of the chymotrypsin family and is closely related to human tissue kallikrein (*1*−*3*). PSA contains 237 amino acids and a single N-linked oligosaccharide (*4*). PSA is primarily expressed in the glandular epithelial cells of the prostate gland and is one of the most abundant proteins in seminal plasma (*5*, *6*). Patients with prostate cancer and benign prostatic hyperplasia often have elevated plasma PSA levels (*7*). PSA is presently used as a tumor marker in diagnosis and management of human prostate cancer. The physiological role of PSA appears to be the liquefaction of the seminal coagulum by proteolysis of semenogelins I and II (*8*−*11*). PSA is also believed to be involved in normal and malignant prostatic cell growth and is implicated in prostatic tumor metastases via the degradation of fibronectin and other matrix proteins (*12*, *13*). These observations suggest that inhibitors of PSA activity may have important clinical applications in the control of prostate cancer growth and metastasis.

Despite the clinical significance of PSA, its protease activity has not been examined thoroughly. PSA displays 10^4−10^6-fold lower activity than that of chymotrypsin under

† This work was supported in part by NIH Grants GM12633 (R.H.A.), HL50366 (L.H.), and DK11011 (A.H.T.) and Training Grant GM07596 (G.F.).

* To whom correspondence should be addressed: Department of Biochemistry, Brandeis University, MS 009, 415 South St., Waltham, MA 02454. E-mail: hedstrom@brandeis.edu. Phone: (781) 736-2333. Fax: (781) 736-2349.

‡ Program in Bioorganic Chemistry, Brandeis University.

§ Present address: Wyeth-Ayerst Research, 401 N. Middletown Rd., Pearl River, NY 10965.

‖ Program in Biochemistry, Brandeis University.

⊥ Present address: Department of Molecular and Cellular Biology, Harvard University, 7 Divinity Ave., Cambridge, MA 02138.

@ Department of Biochemistry, Brandeis University.

Present address: Nichols Institute Diagnostics, 33047 Calli Aviador, San Juan Capistrano, CA 92675.

○ Harvard School of Public Health.

+ Deceased June 18, 2000. This paper is dedicated to his memory. His enthusiasm, insights, and unique perspective were an inspiration to many, and his presence is greatly missed.

[1] Abbreviations: PSA, prostate specific antigen; rh-PSA, recombinant human PSA; Suc, succinyl; AMC, 7-amino-4-methylcoumarin; CK, chloromethyl ketone; DFP, diisopropyl fluorophosphate; TPCK, L-1-*p*-tosylamino-2-phenylethyl chloromethyl ketone; IPTG, isopropyl β-D-thiogalactopyranoside; Bz, benzoyl; DTT, dithiothreitol; CD, circular dichroism.

10.1021/bi010364j CCC: $20.00
Published on Web 09/08/2001

conventional in vitro assay conditions (*3*, *8*, *14*, *15*). The heterogeneity of PSA and the presence of contaminating proteases continue to complicate the characterization of this protein (*16*−*18*). Moreover, while DFP and peptidyl chloromethyl ketones are potent inactivators of most serine proteases, these compounds react slowly with PSA. The reasons for the low protease activity of PSA are not understood.

We have expressed human PSA in *Escherichia coli* to characterize the protease activity of the protein. We have found that the activity of PSA is increased 1000-fold in the presence of high salt concentrations and that the structure of PSA becomes more compact under these conditions. Interestingly, human prostatic fluid contains from 150- to 1000-fold higher citrate concentrations than prostatic stromal tissue (*19*). Thus, this salt activation phenomenon may regulate PSA activity in vivo.

MATERIALS AND METHODS

Materials. The full-length *c*DNA clone of human PSA (pGEM3PSA) (*2*) was kindly provided by A. Lundwall of Malmo General Hospital (Malmo, Sweden). *E. coli* expression vector pT7-7 was a gift from S. Tabor (Harvard Medical School, Boston, MA). Suc-Ala-Ala-Pro-Phe-CK was purchased from Enzyme System Products. Monoclonal anti-(human PSA) mouse IgG was purchased from ICN. Enterokinase was purchased from Biozyme. Native human PSA was obtained from Novabiochem and Calbiochem. DFP was purchased from Aldrich. IPTG, Triton X-100, guanidine hydrochloride, TPCK, and Suc-Ala-Ala-Pro-Phe-AMC were purchased from Sigma.

Vector Construction. The PSA coding sequence was amplified by PCR from pGEM3PSA using *Pfu* DNA polymerase with primers containing *Eco*RI and *Sal*I restriction sites and the sequence encoding an enterokinase cleavage site at the N-terminus of mature PSA. The PCR fragment was ligated into vector pT7-7 to create pT7-7-PSA. The sequence of PSA was verified using the PRISM dye deoxy terminator cycle sequencing method (Applied Biosystems, Inc.). pT7-7-PSA was transformed into *E. coli* strain BL21. The expected sequence (ATG GCT AGA ATT CCT AGG GAC GAC GAC GAT AAG ATT) was observed, confirming the presence of the engineered N-terminus (Met-Ala-Arg-Ile-Pro-Arg-Asp-Asp-Asp-Lys-**Ile**, where **Ile** is the first residue in mature PSA).

Expression, Purification, and Refolding of Recombinant PSA. PSA expression was induced with the addition of 0.1 mM IPTG at an OD_{590} of 0.5, and the culture was incubated for 4 h at 37 °C. The cells were harvested by centrifugation, washed with a 0.85% NaCl solution, and then lysed by sonication in 50 mM Tris-HCl (pH 8), 10 mM EDTA, and 5% sucrose. Inclusion bodies were harvested by centrifugation. The pellet contained rh-PSA and one other major protein as detmined by SDS−PAGE. The contaminating protein was removed by washing with Triton X-100. The resulting pellet was washed twice with H_2O and dissolved in 100 mL of 50 mM Tris-HCl (pH 8), 10 mM EDTA, 6 M guanidine-HCl, and 10 mM DTT. The solution was adjusted to a final protein concentration of 0.3 mg/mL and diluted 10-fold into 50 mM Tris-HCl (pH 8), 10 mM EDTA, and 5 mM L-cysteine. The solution was stirred at 4 °C for 24 h and then concentrated by ultrafiltration to 0.3 mg/mL. The protein was subsequently dialyzed against 25 mM MES, 2 mM $CaCl_2$ (pH 6), 0.1% Triton X-100, and 5 mM L-cysteine, followed by two changes of 25 mM MES, 2 mM $CaCl_2$ (pH 6), and 0.1% Triton X-100. SDS−PAGE demonstrated a purity of >95% rh-PSA under both reducing and nonreducing conditions, indicating that renaturation results in a single folded species. rh-PSA was activated with 5 μg of enterokinase. The enzyme was further concentrated to 1−2 mg/mL and transferred to 50 mM HEPES (pH 8.0) by dialysis. rh-PSA was routinely stored at −20 °C with 50% glycerol. The rh-PSA concentration was based on the absorbance at 280 nm and a calculated extinction coefficient of 1.75. This value is in close agreement with that previously determined experimentally (*20*), as well as enzyme concentrations obtained using the method of Bradford (*21*).

Assay of Enzymatic Activity. The hydrolysis of fluorogenic substrates was monitored on a Hitachi F-2000 fluorescence spectrophotometer with excitation at 380 nm and emission at 460 nm. The hydrolysis of *p*-nitroanilide substrates (Sigma) was monitored by the absorbance at 410 nm. Assays were performed at 25 °C in 50 mM Tris-HCl (pH 7.8) and 100 mM NaCl with Suc-Ala-Ala-Pro-Phe-AMC (Bachem) as the substrate except where otherwise specified. The k_{cat}/K_m for this substrate under these conditions was 0.64 M^{-1} s^{-1}. The Bz-Lys-Val-Phe-AMC substrate was synthesized using conventional solution peptide chemistry. Bz-Lys-Val-Phe-AMC: ^{1}H NMR ($CDCl_3$) δ 8.70 (s, 1), 7.14−8.0 (m, 12), 6.42 (m, 1), 6.18 (s, 1), 4.87 (m, 1), 4.75 (m, 1), 4.37 (t, 1), 3.87 (t, 2), 3.15 (t, 2), 2.38 (s, 3), 1.40 (m, 6), 0.95 (d, 3), 0.80 (d, 3). The proteolytic activity was also measured qualitatively by a nonreducing SDS−PAGE casein gel. A 15% SDS−PAGE gel with a casein content of 2 mg/mL was prepared. A 1:1 mixture of PSA and 2× nonreducing sample buffer was loaded without preboiling. After electrophoresis, the protein gel was washed in 2.5% Triton X-100 for 45 min and then gently shaken overnight at room temperature in 50 mM Tris-HCl (pH 7.0) and 10 mM $CaCl_2$ before routine staining and destaining. A light halo surrounding the rh-PSA band demonstrated the digestion of casein.

Inactivation of rh-PSA. rh-PSA (10 μM) was incubated at room temperature with varying concentrations of known serine protease inhibitors (DFP, TPCK, and Suc-Ala-Ala-Pro-Phe-CK) in 50 mM Tris-HCl (pH 7.8) in the presence or absence of 0.9 M Na_2SO_4, conditions found to be favorable for substrate and inhibitor solubility and stability. Aliquots were assayed for activity at appropriate intervals. The resulting fraction of activity was plotted against time on a semilog plot to yield the apparent inactivation rate constant k_{app}. Azapeptide inactivation was monitored by diluting PSA into a cuvette containing inhibitor, 1 M potassium phosphate (pH 7.0), and 4.5 mM Suc-Ala-Ala-Pro-Phe-pNA under these conditions (k_{cat} = 0.35 s^{-1} and K_m = 3.6 mM). The values of k_{obs} were determined by fitting the progress curves to the equation $A(t) = A_o + V_i(1 - e^{-k_{obs}t})/k_{obs}$, where A is the absorbance at 410 nm at time t, A_o is the absorbance at time zero, V_i is the initial velocity, and k_{obs} is the observed first-order rate constant. The values of K_i and k_{inact} were determined from the secondary plot relationship $k_{obs} = k_{inact}[I]/K_{i\ app} + [I]$, where $K_{i\ app}$ is the apparent inhibition constant. The true K_i was determined from the relationship $K_i = K_{i\ app}/(1 + [S]/K_m)$. The values for k_{off} were determined by inactivating 50 μg of PSA and separating the EI complex

from free inhibitor using a 1 mL Penefsky column. The eluate was assayed for activity over a 5 h time period. The value of k_{off} was determined by plotting the percent inhibition versus time and fitting the result to a first-order exponential.

Size Filtration Chromatography. A Superose 6 column (Pharmacia) was equilibrated with 50 mM Tris-HCl (pH 7.8) or 50 mM Tris-HCl (pH 7.8) and 0.5 M Na_2SO_4. Protein samples were incubated in the absence or presence of 0.5 M Na_2SO_4 for 10 min and then applied to the corresponding equilibrated column. The samples were eluted at a rate of 0.5 mL/min with the same buffer used for equilibration. The elution was monitored at 280 nm.

Circular Dichroism Studies. CD measurements were performed at room temperature on a Jobin-Yvon Mark V Autodichrograph. The spectra were collected in the near-UV range (320−240 nm) using a 1 cm path length cell with a sensitivity of 5×10^{-6} and a response time of 1 s at 0.2 nm intervals. All samples contained 0.2 mg/mL rh-PSA in 10 mM HEPES (pH 8). Spectra were monitored in the presence or absence of 0.5 M Na_2SO_4. These conditions were chosen to maximize PSA solubility and minimize sample handling.

Analytical Ultracentrifugation. The molecular mass of rh-PSA was evaluated under different buffer conditions using a Beckman XL-A analytical ultracentrifuge by sedimentation equilibrium analysis. PSA was examined at two concentrations in the absence of salt (31 and 67 μM) and in the presence of 0.5 M Na_2SO_4 (27 and 46 μM). The data were collected at 9000 rpm at 20 °C and analyzed with the XL-A software provided by Beckman using the single-ideal species model. The partial specific volume ($\bar{v}$) of rh-PSA in 50 mM HEPES (pH 7.8) was calculated to be 0.744 using the method of Cohn and Edsall (*22*). The $\bar{v}$ for rh-PSA in 0.5 M Na_2SO_4 was adjusted to 0.762 as a result of a correction applied as previously described (*23*) using interaction parameters for 0.5 M Na_2SO_4 (*24*). The densities of 50 mM Tris (pH 7.8) (1.008 g/mL) and the same buffer containing 0.5 M Na_2SO_4 (1.069 g/mL) were measured.

Dynamic Light Scattering. DLS studies were performed using the DynaPro LSR instrument from Protein Solutions. The partial specific volumes described for the analytical ultracentrifugation experiment were used. Values for refractive indices and the viscosity of citrate solutions were from the literature (*25*). The viscosities of the sulfate solutions were measured with a Cannon A334 viscometer. The analysis was preformed using the Dynamics software provided with the instrument, and data were fitted using the volume shape hydration model and a frictional ratio for an average 24−110 kDa protein provided by the program. Experiments were conducted with 55 μM rh-PSA [50 mM HEPES (pH 7.8)], 38 μM rh-PSA [50 mM HEPES, 16 mM Tris, and 0.5 M Na_2SO_4 (pH 7.8)], and 38 μM rh-PSA [16 mM HEPES and 0.5 M citrate (pH 6.8)].

N-Terminal Sequencing and Mass Spectrometry. N-Terminal sequence determination and MALDI mass spectrometry were performed at the peptide facility of the Department of Physiology, Tufts University School of Medicine (Boston, MA).

RESULTS

Expression of Human PSA in E. coli. PSA was subcloned into vector pT7-7 and expressed in *E. coli* BL21 cells as a zymogen containing an N-terminal extension. A similar PSA expression system has been reported elsewhere (*20*). Recombinant PSA accumulated exclusively in inclusion bodies. It was purified, solubilized, and refolded using the procedures described in Materials and Methods. The resulting protein was >98% pure as judged by SDS−PAGE. Mature recombinant PSA (rh-PSA) was obtained by removing the N-terminal extension with enterokinase. The N-terminus was verified by amino acid sequencing. The typical yield was 6 mg of purified rh-PSA per liter of culture. rh-PSA reacted with mouse monoclonal anti-human PSA antibody and exhibited chymotrypsin-like substrate specificity as previously reported (*1*, *3*, *18*). rh-PSA has no detectable trypsin-like activity. To ensure that the protease activity was not due to contaminating proteases, a nonreducing SDS−PAGE casein gel was prepared as described in Materials and Methods. Casein digestion occurred exclusively at the PSA band, indicating that the protease activity observed is not likely to be due to contaminating proteases (data not shown). rh-PSA is also inhibited by α1-antichymotrypsin, forming a 78 kDa complex as previously observed for human seminal PSA (data not shown) (*1*, *20*). Incubation of PSA with excess α1-antichymotrypsin indicated that ∼70% of the rh-PSA is active as determined by examination of Coomassie-stained gels. Similar active fractions of recombinant PSA preparations have been reported in other laboratories (*1*, *26*). The specific activity of rh-PSA (0.5 μmol min^{-1} mg^{-1}) is similar to that of human seminal PSA (0.34 μmol min^{-1} mg^{-1}) as monitored by the hydrolysis of 0.2 mM Bz-Lys-Val-Phe-AMC in the absence of salt. Takayama and co-workers also reported comparable activities for rh-PSA and seminal PSA (*20*). These observations indicate that glycosylation is not required for proteolytic activity. The hydrolysis of Bz-Lys-Val-Phe-AMC by rh-PSA displays typical Michaelis−Menten kinetics (k_{cat} = 0.0014 s^{-1} and K_m = 0.86 mM). However, the commercially available substrate Suc-Ala-Ala-Pro-Phe-AMC (k_{cat}/K_m = 640 M^{-1} s^{-1}) used in the following experiments does not exhibit saturable kinetics.

PSA Activity Increases in the Presence of Salt. In the course of characterizing PSA, we observed that protease activity increased in high salt concentrations. The magnitude of this effect is highly dependent on the nature of the anion (Figure 1); the nature of the cation has only a modest effect on PSA activity (Table 1). PSA is >10^3-fold more active in the presence of 1.3 M Na_2SO_4, and the overall anion effect follows the Hofmeister series when normality is considered (Figure 1) (*27*): SO_4^{2-} ≈ citrate > Ac^- > Cl^- > Br^- > I^-. The activity of native PSA also increases in the presence of salt (Figure 2, compare panels A and B). While native PSA and rh-PSA have similar activities under low-salt conditions, native PSA is approximately 2-fold more active than rh-PSA under high-salt conditions. This observation suggests that glycosylation may modulate salt activation.

The Rate of Inactivation of PSA Increases in the Presence of Salt. Serine proteases are inactivated by DFP and peptidyl chloromethyl ketones. DFP (2 mM) inactivates rh-PSA in a first-order process under conditions of low ionic strength. The rate of inactivation increases 30-fold (from 0.0042 to 0.12 s^{-1}) in the presence of 0.9 M Na_2SO_4. The molecular mass of DFP-inactivated rh-PSA determined by MALDI mass spectrometry is 26 276 ± 26 Da, which agrees with the theoretical mass of 26 254 Da for PSA modified by a

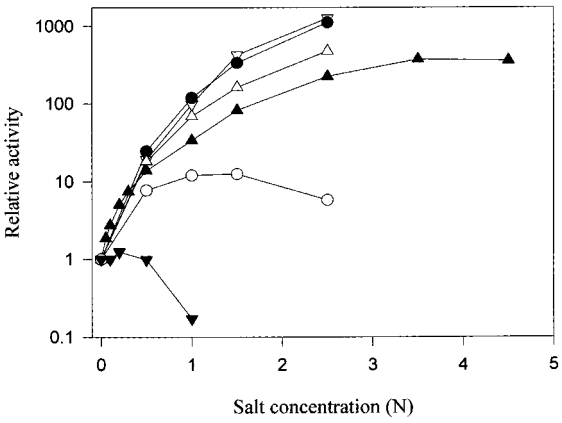

FIGURE 1: Effect of anions on rh-PSA activity. rh-PSA (11 nM) was assayed with 125 μM Suc-Ala-Ala-Pro-Phe-AMC in 50 mM Tris-HCl (pH 7.8) containing 0.5, 1.0, 1.5, or 2.5 N sodium citrate (▽), Na_2SO_4 (○), and NaOAc (△); 0.05, 0.1, 0.2, 0.3, 0.5, 1.0, 1.5, 2.5, 3.5, or 4.5 N NaCl (▲); 0.5, 1, 1.5, or 2.5 N NaBr (●); and 0.1, 0.2, 0.5, or 1.0 N NaI (▼).

Table 1: Sulfate Activation of rh-PSA[a]

	Na_2SO_4	Li_2SO_4	$(NH_4)_2SO_4$	K_2SO_4	$MgSO_4$
relative activity	1	0.87	0.84	0.72	0.70

[a] Assays were performed in 50 mM Tris buffer containing the indicated salts (0.5 M) at pH 7.8 and 25 °C.

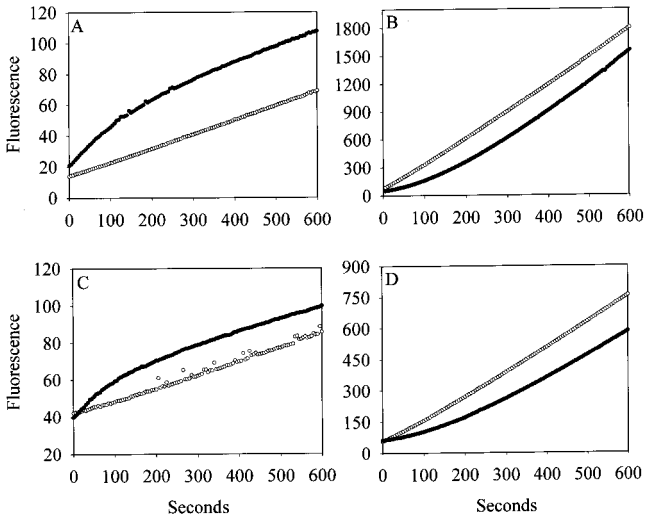

FIGURE 2: Effect of 0.8 M Na_2SO_4 on the time course of product formation. All reaction mixtures contained 125 μM Suc-Ala-Ala-Pro-Phe-AMC and 50 mM Tris-HCl (pH 7.8). PSA (A) or rh-PSA (C) (1.1 μM) was preincubated for 10 min at 25 °C with 0.8 M Na_2SO_4 and then added to assay buffer containing substrate (●). The final concentration of Na_2SO_4 was 38 mM. In the control experiment (○), enzyme was added to initiate a reaction in assay buffer containing 38 mM Na_2SO_4. PSA (B) or rh-PSA (D) (11 nM) was added to initiate a reaction in assay buffer containing 0.8 M Na_2SO_4 (●). In a parallel experiment, the substrate was added to initiate a reaction in assay buffer containing enzyme and 0.8 M Na_2SO_4 (○).

diisopropyl phosphate moiety. In contrast to DFP, TPCK and Suc-Ala-Ala-Pro-Phe-CK do not inactivate rh-PSA under low-salt conditions. The rate of inactivation by Suc-Ala-Ala-Pro-Phe-CK (2 mM) increases by at least 20-fold to 0.021 s^{-1} in the presence of 0.9 M Na_2SO_4. However, no inactivation of rh-PSA by TPCK is observed even in the presence of high salt.

Table 2: Azapeptide Inhibition of rh-PSA[a]

azapeptide	K_i (μM)	k_{inact} (s^{-1})	k_{inact}/K_i (M^{-1} s^{-1})
1	64	1.8×10^{-3}	31
2	41	1.7×10^{-2}	410
3	5	1.3×10^{-2}	2600
4	0.5	1.5×10^{-2}	32000

[a] See Figure 3 for structures. Azapeptide inactivation was monitored by diluting PSA into a cuvette containing inhibitor, 1 M potassium phosphate (pH 7.0), and 4.5 mM Suc-Ala-Ala-Pro-Phe-pNA at 25 °C.

Azapeptide Inhibitors of PSA. Azapeptides inhibit cysteine and serine proteases (*28*−*30*). Azapeptides undergo the same reaction as a peptide substrate. However, when the aza-amino acid is in the P_1 position, the resulting acyl−enzyme intermediate is stable. The results cited above suggested that azapeptides might inhibit PSA under high-salt conditions. We screened our collection of azapeptides and discovered that *N*-acetyl-L-Phe-azaGly-phenyl ester inhibits rh-PSA at a concentration of 50 μM. Slow binding kinetics are observed, and the activity approaches zero (data not shown). The potency of this lead compound was increased by optimizing S−P interactions (nomenclature of ref *31*). PSA reportedly has a strong preference for substrates with Tyr in the P_1 position, and the following preferences in the other subsites: Ser in P_3 and Tyr > Val/Leu/Phe in P_2 (*32*). As expected, AzaTyr is preferred over aza-Phe in the P_1 position of the inhibitor by 12-fold as measured by k_{inact}/K_i (Figure 3 and Table 2). The introduction of Boc-L-Ser at the P_3 position increases the value of k_{inact}/K_i by a factor of 80. Both compounds **3** and **4** produce stable acyl−enzyme intermediates that hydrolzye slowly, resulting in half-lives of 4.4 and 3.8 h, respectively.

The Conformation of PSA Changes in the Presence of 0.8 M Na_2SO_4. The following observations suggest that the anion effect is the result of a change in PSA conformation and not a nonspecific effect from "salting out" the substrate. A lag in activity was observed when assays containing 0.8 M Na_2SO_4 were initiated by the addition of either rh-PSA or native PSA [Figure 2A,C (circles)]. However, no lag was observed when either enzyme was incubated in 0.8 M Na_2SO_4, and the assay was initiated by the addition of substrate [Figure 2A,C (triangles)]. These observations suggest that PSA undergoes a slow conformational change in the presence of SO_4^{2-}.

This hypothesis predicts that when PSA is preincubated in the presence of SO_4^{2-} and diluted into an assay mix at a low ionic strength, the protein will slowly convert to the less active conformation. Therefore, a rapid initial phase of substrate hydrolysis should be observed, followed by a slower steady-state rate when the protein has relaxed to the less active conformation. This prediction is confirmed. A significant rapid phase is observed when PSA is preincubated with 0.8 M Na_2SO_4 at 25 °C [Figure 2B,D (triangles)]. No rapid phase is seen when enzyme is preincubated under low-salt conditions [Figure 2B,D (circles)].

The Structure of PSA Changes in the Presence of SO_4^{2-}. The near-UV CD spectra of rh-PSA in the presence and absence of 0.5 M Na_2SO_4 are significantly different (Figure 4). In the absence of SO_4^{2-}, the spectrum shows little negative ellipticity between 250 and 320 nm, indicating few tertiary interactions are present in PSA (*33*, *34*). However, in the presence of SO_4^{2-}, the CD spectrum of rh-PSA exhibits

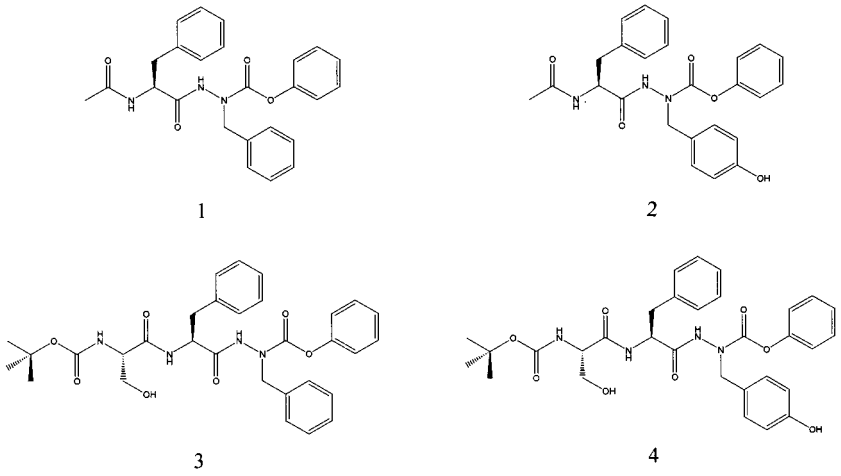

FIGURE 3: Azapeptide inhibitors.

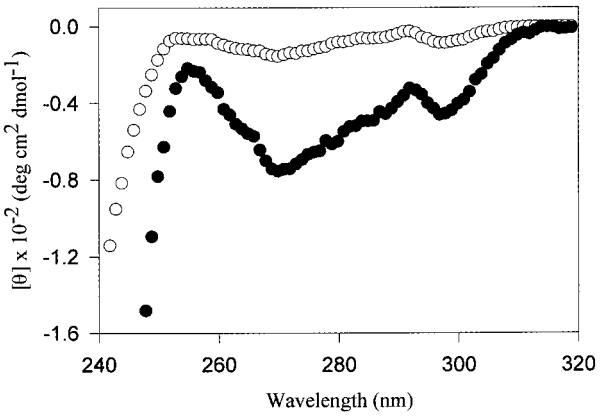

FIGURE 4: Near-UV CD spectra of rh-PSA in the absence (○) and presence (●) of 0.5 M Na_2SO_4. The measurements were performed as described in Materials and Methods.

deep troughs at 270 and 300 nm. Tryptophan and tyrosine side chains are the major contributors to near-UV CD (*35*). This result suggests that these aromatic residues exhibit restricted solvent accessibility in the presence of SO_4^{2-}.

PSA Remains Monomeric in the Presence of Salt. Anions such as citrate and SO_4^{2-} are known to promote nonpolar interactions in proteins (*36*). Proteins are consequently more likely to associate (*37*, *38*). Therefore, the salt activation of PSA could result from the formation of dimers or higher-order multimers. The salt activation of hCMV and HSV proteases results from such a dimerization mechanism (*39*−*42*). To test this hypothesis, PSA was eluted from a Superose 6 size filtration column in the presence or absence of 0.5 M Na_2SO_4 as described in Materials and Methods. In the absence of Na_2SO_4, PSA eluted at 32.3 min, between ribonuclease A (14 kDa, 37.8 min) and ovalbumin (43 kDa, 26.9 min) (Figure 5). In the presence of 0.5 M Na_2SO_4, the elution of ribonuclease A was unchanged (37.2 min) and the elution time of ovalbumin increased by 3.5 min (Figure 5). However, the elution time of PSA increased to 38.2 min. An increase in elution time is inconsistent with the formation of a dimer but does suggest that PSA may adopt a more compact conformation under high-salt conditions (*43*). Alternatively, the increase in elution time could also indicate that rh-PSA interacts with the gel matrix in the presence of salt as has been observed with other proteins (*44*). Therefore,

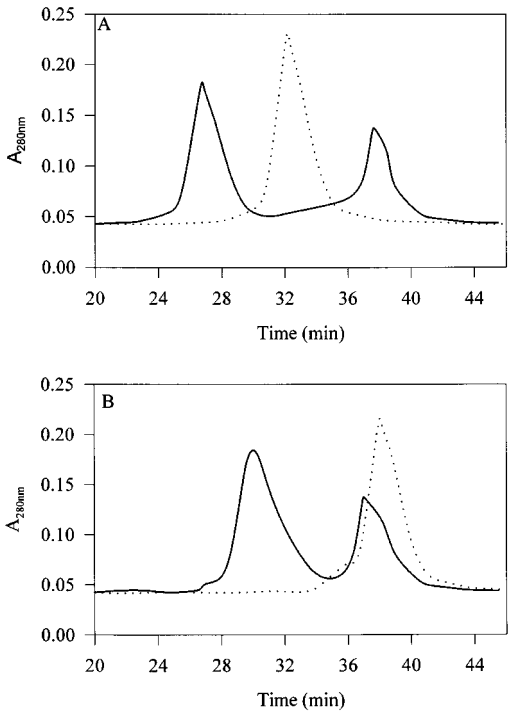

FIGURE 5: Elution profiles of rh-PSA from size filtration chromatography. (A) Molecular markers ribonuclease A and ovalbumin (0.4 mg each) were injected onto a Superose column equilibrated with 50 mM Tris-HCl (pH 7.8) (—). rh-PSA (0.1 mg) was similarly injected and eluted (···). (B) As for panel A, but the column was equilibrated and eluted with 50 mM Tris-HCl (pH 7.8) and 0.5 M Na_2SO_4. Ribonuclease A and ovalbumin (—) or rh-PSA (···).

we used analytical centrifugation methods to determine the quaternary structure of PSA.

Sedimentation equilibrium experiments show that the apparent molecular mass of rh-PSA in the absence of salt (28.3 kDa) is not significantly different from that determined in the presence of 0.5 M Na_2SO_4 (26.5 kDa) when comparing the results from two different concentrations of rh-PSA (Figure 6). A slight deviation between the data and the model is observed in Figure 6 (panels C and D) at higher absorbance values. Examination of the $M_{w,app}$ versus enzyme concentration plot revealed that $M_{w,app}$ decreases at higher protein concentrations (data not shown). This has been previously described for hCMV protease (*45*), and was attributed to positive thermodynamic nonideality.

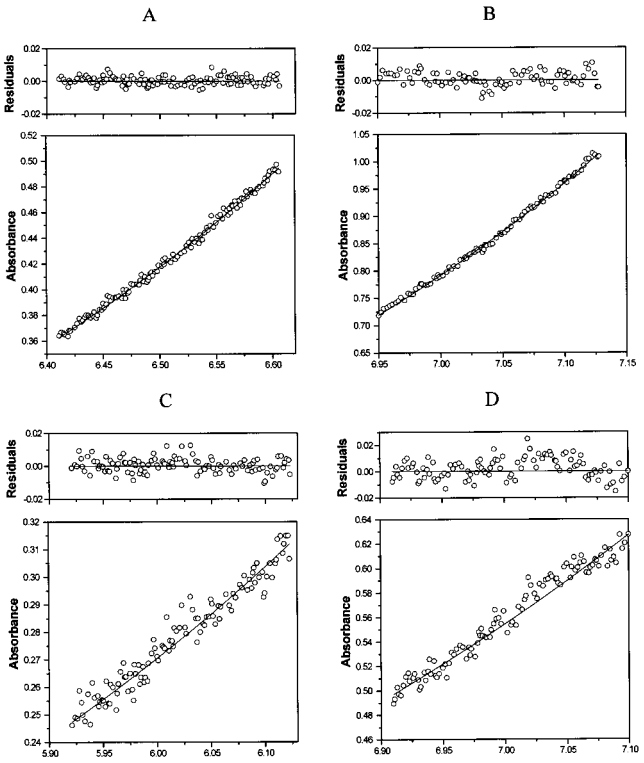

FIGURE 6: Equilibrium sedimentation of rh-PSA. The data were collected at 9000 rpm at 20 °C and analyzed as described in Materials and Methods. Samples of rh-PSA in 50 mM Tris (pH 7.8) in the absence (A and B) or presence (C and D) of 0.5 M Na_2SO_4 and molecular mass determination results: (A) 27 μM rh-PSA (28 096 ± 1289 Da), (B) 46 μM rh-PSA (24 877 ± 807.4 Da), (C) 30 μM rh-PSA (26 741 ± 328.5 Da), and (D) 67 μM rh-PSA (29 994 ± 270 Da).

Table 3: Dynamic Light Scattering of Native and rh-PSA[a]

	additive	radius	MW (kDa)	polydispersity (%)
rh-PSA	500 mM citrate	2.489	26	48
rh-PSA	480 mM Na_2SO_4	2.577	29	48
rh-PSA	none	2.439	25	49

[a] Experiments were conducted with 55 μM rh-PSA [50 mM HEPES (pH 7.8)] or 38 μM rh-PSA [50 mM HEPES, 16 mM Tris, and 0.5 M Na_2SO_4 (pH 7.8) and 16 mM HEPES and 0.5 M citrate (pH 6.8)].

Dynamic light scattering was also utilized to evaluate the possibility of PSA dimerization. Table 3 shows that the apparent MW of rh-PSA does not increase under high-salt conditions. This observation indicates that the activation of PSA does not involve dimerization. Polydispersity is noted to be high under all three conditions (48−49%) and could indicate the presence of several species of rh-PSA. While increased polydispersity has been seen in conjunction with oligomerization (*40*), this has also been noted for the β-lactamase monomer (*46*).

DISCUSSION

PSA and Prostate Disease. The role of PSA in prostate cancer and benign prostatic hyperplasia is unknown. PSA may be directly involved in the cell proliferation process via cleavage of insulin-like growth factor 3 binding protein 3 (IGFBP-3) (*47*). The resulting IGFBP-3 fragments are unable to bind and sequester insulin-like growth factor 1 (IGF-1), thus releasing a potent mitogen (*12*). Inhibition of PSA may provide a treatment for prostate disease. Elucidation of the mechanism of regulation of PSA activity will enable the development of more specific and potent inhibitors of this enzyme.

PSA Specificity. The substitution of Tyr for Phe in the P_1 position of the azapeptide resulted in a 12-fold increase in k_{inact}/K_i (Figure 3). This is consistent with several independent observations. PSA exhibits specificity for a P_1 Tyr residue in semenogelins I and II (*48*), and the site of cleavage of IGFBP-3 by PSA has been recently determined to be at Tyr^{159} (*49*). Identification of peptide substrates using the phage display technique has also indicated a preference for a P_1 Tyr (*32*).

Salt Activates PSA. We observe that SO_4^{2-} and citrate enhance the protease activity of PSA by 1000-fold. Salt activation is also observed with native glycosylated PSA. The inhibition of PSA by DFP, CK, and azapeptides is similarly accelerated. This activation is strongly anion-dependent and follows the Hofmeister series. Activation was independent of the nature of the cation under our assay conditions. Unfortunately, we are unable to determine the effect of salt concentrations on Michaelis−Menten parameters due to experimental constraints (the substrate solubility is too low to permit concentrations in excess of the value of K_m under both low- and high-salt conditions).

While the manuscript was in preparation, Cooperman and Hsieh published a description of the salt activation of PSA (*26*). However, unlike our work, these authors observed only a 10-fold increase in activity. Further, activation was reported to be cation-dependent with NaCl as the strongest activator. This discrepancy may result from the use of reactive *p*-nitroanilide substrates in the Cooperman experiments. Reactive substrates frequently mask catalytic lesions in mutant serine proteases (*50*).

Mechanism of Salt Activation of PSA. Salt-induced increases in protease activity have been previously observed with HSV type I protease and hCMV protease (*39*−*42*). In both cases, increases in salt concentration promote formation of an active protease dimer. PSA remains monomeric at high salt concentrations as indicated by size exclusion chromatography, sedimentation equilibrium, and dynamic light scattering experiments. Thus, PSA activation does not involve dimer formation and must occur by a distinct mechanism. CD spectroscopy indicates that PSA undergoes a conformational change under high-salt conditions. The active conformation is likely to be more compact than the inactive conformation as suggested by the retardation of PSA elution during size exclusion chromatography experiments and the more constrained movement of aromatic residues indicated by CD spectroscopy. Interestingly, the ellipticity at 270 nm (0.8×10^{-2} deg cm^2 dmol^{-1}) is similar to the ellipticity at 277 nm observed for bovine trypsin (1.0×10^{-2} deg cm^2 dmol^{-1}) (*51*). The interconversion of the inactive and active conformations of PSA is slow, resulting in the burst and lag phases illustrated in Figure 2. Christianson et al. also observed a rapid phase of substrate hydrolysis when PSA, stored at a low ionic strength at 4 °C, is diluted into assay mix in the absence of SO_4^{2-} (*1*). The origin of the rapid phase in Christensson's experiments is unclear. We have observed a similar rapid phase when a cold enzyme solution is diluted into assay buffer. This rapid phase is not observed when the enzyme solution is pre-equilibrated at room temperature (Figure 2B,D). These observations suggest

that low temperature also favors the active conformation of PSA.

Thermodynamic Basis for Regulation of PSA Activity by Salts. The in vitro activation of the enzyme by high concentrations of salt, following the Hofmeister series, suggests that the regulation is exercised by a totally general nonspecific thermodynamic solvent effect, namely, the preferential exclusion of the salt from the surface of the protein. Since this interaction is thermodynamically unfavorable, the system will tend to reduce it by driving the protein to the more compact active conformation, in which the solvent−protein surface area of the contact is reduced. The activator (salt) acts, therefore, by not coming into contact with the molecule that it activates. The thermodynamic details are presented in the Appendix.

Implications for in Vivo Regulation of PSA Activity. The citrate concentration in human prostatic fluid is as high as 150 μmol citrate/g wet weight, which is 150−1000-fold higher than the concentration found in prostatic stromal tissue. Prostatic fluid also contains abundant free amino acids and proteins which might exert a similar effect. Thus, changes in anion concentration may regulate PSA activity in *vivo*.

ACKNOWLEDGMENT

We thank Bhupesh Kapoor for synthesizing compound **2** and S. N. Timasheff for helpful discussions.

SUPPORTING INFORMATION AVAILABLE

Syntheses and characterization of azapeptide inhibitors. This material is available free of charge via the Internet at http://pubs.acs.org.

REFERENCES

1. Christensson, A., Laurell, C.-B., and Lilja, H. (1990) *Eur. J. Biochem. 194*, 755−763.
2. Lundwall, A., and Lilja, H. (1987) *FEBS Lett. 214*, 317−322.
3. Watt, K. W. K., Lee, P.-J., M'Timkulu, T., Chan, W.-P., and Loor, R. (1986) *Proc. Natl. Acad. Sci. U.S.A. 83*, 3166−3170.
4. Belanger, A., van Halbeek, H., Gravees, H. C. B., Grandbois, K., Stamey, T. A., Huang, L., Poppe, I., and Labrie, F. (1995) *Prostate 27*, 187−197.
5. Lilja, H., and Abrahamsson, P. A. (1988) *Prostate 12*, 29−38.
6. Sinha, A. A., Wilson, M. J., and Gleason, D. F. (1987) *Cancer 60*, 1288−1293.
7. Oesterling, J. E. (1991) *J. Urol. 145*, 907−923.
8. Lilja, H. (1985) *J. Clin. Invest. 76*, 1899−1903.
9. Lilja, H., and Lundwall, A. (1992) *Proc. Natl. Acad. Sci. U.S.A. 89*, 4559−4563.
10. Lilja, H., Oldbring, J., Ranncvik, G., and Laurell, C.-B. (1993) *J. Clin. Invest. 80*, 281−285.
11. Robert, M., and Gagnon, C. (1999) *Cell. Mol. Life Sci. 55*, 944−960.
12. Sutkowski, D. M., Goode, R. L., Baniel, J., Teater, C., Cohen, P., McNulty, A. M., Hsiung, H. M., Becker, G. W., and Neubauer, B. L. (1999) *J. Natl. Cancer Inst. 91*, 1663−1669.
13. Webber, M. M., Wahgray, A., and Bells, D. (1995) *Clin. Cancer Res. 1*, 1089−1094.
14. Denmeade, S. R., Lou, W., Lovgren, J., Malm, J., Lilja, H., and Isaacs, J. T. (1997) *Cancer Res. 57*, 4924−4930.
15. Schaller, J., Akiyama, K., Tsuda, R., Hara, M., Marti, T., and Rickli, E. E. (1987) *Eur. J. Biochem. 170*, 111−120.
16. Frenette, G., Tremblay, R. R., Lazure, C., and Dube, J. Y. (1997) *Int. J. Cancer 71*, 897−899.
17. Wang, M. C., Loor, R. M., Li, S. L., and Chu, T. M. (1982) *Methods Cancer Res. 19*, 179−197.
18. Yoshida, E., Ohmura, S., Sugiki, M., Maruyama, M., and Mihara, H. (1995) *Int. J. Cancer 63*, 863−865.
19. Costello, L. C., Franklin, R. B., and Narayan, P. (1999) *Prostate 38*, 237−245.
20. Takayama, T. K., Fujikawa, K., and Davie, E. W. (1997) *J. Biol. Chem. 272*, 21582−21588.
21. Bradford, M. M. (1976) *Anal. Biochem. 72*, 248−254.
22. Cohn, E. J., and Edsall, J. T. (1943) in *Proteins, Amino Acids and Peptides*, pp 370, Van Nostrand-Rheinhold, Princeton, NJ.
23. Arakawa, T., and Timasheff, S. N. (1985) *Methods Enzymol. 117*, 60−65.
24. Arakawa, T., and Timasheff, S. N. (1982) *Biochemistry 21*, 6545−6552.
25. Lide, D. R., and Frederikse, H. P. R., Eds. (1997) *CRC Handbook of Chemistry & Physics*, 78th ed.; pp 57, CRC Press, Boca Raton, FL.
26. Hsieh, M., and Cooperman, B. S. (2000) *Biochim. Biophys. Acta 1481*, 75−87.
27. Hofmeister, F. (1888) *Arch. Exp. Pathol. Pharmakol. 24*, 247.
28. Baggio, R., Shi, Y.-Q., Wu, Y.-Q., and Abeles, R. H. (1996) *Biochemistry 35*, 3351−3353.
29. Magrath, J., and Abeles, R. H. (1992) *J. Med. Chem. 35*, 4279−4283.
30. Powers, J. C., Boone, R., Carroll, D. L., Gupton, B. F., Kam, C. M., Nishino, N., Sakamoto, M., and Tuhy, P. M. (1984) *J. Biol. Chem. 259*, 4288−4294.
31. Schechter, I., and Berger, A. (1967) *Biochem. Biophys. Res. Commun. 27*, 157−162.
32. Coombs, G. S., Bergstrom, R. C., Pellequer, J. L., Baker, S. I., Navre, M., Smith, M. M., Tainer, J. A., Madison, E. L., and Corey, D. R. (1998) *Chem. Biol. 5*, 475−488.
33. Dolgikh, D. A., Abaturov, L. V., Bolotina, I. A., Brazhnikov, E. V., Bychkova, V. E., Bushuev, V. N., Gilmanshin, R. L., Lebedev, Y. O., Semisotnov, G. V., Tiktopulo, E. I., and Ptityn, O. B. (1985) *Eur. Biophys. J. 13*, 109−121.
34. Nozaka, M., Kuwajima, K., Nitta, K., and Sugai, S. (1978) *Biochemistry 17*, 3753−3758.
35. Adler, A. J., Greenfield, N. J., and Fasman, G. D. (1973) *Methods Enzymol. 27*, 675−735.
36. Nandi, P. K., and Robinson, D. R. (1972) *J. Am. Chem. Soc. 94*, 1308−1315.
37. Jencks, W. P. Y. (1987) *Catalysis in Chemistry and Enzymology*, Dover, New York.
38. von Hippel, P. H., and Schleigh, T. (1969) *Acc. Chem. Res. 2*, 257−265.
39. Darke, P. L., Cole, J. L., Waxman, L., Hall, D. L., Sardana, M. K., and Kuo, L. C. (1996) *J. Biol. Chem. 271*, 7445−7449.
40. Margosiak, A. A., Vanderpool, D. L., Sisson, W., Pinko, C., and Kan, C.-C. (1996) *Biochemistry 35*, 5300−5307.
41. Schmidt, U., and Darke, P. L. (1997) *J. Biol. Chem. 272*, 7732−7735.
42. Hall, D. L., and Darke, P. L. (1995) *J. Biol. Chem. 270*, 22697−22700.
43. Washabaugh, M. W., and Collins, K. D. (1986) *J. Biol. Chem. 261*, 12477−12485.
44. Westerlund, J., and Yao, Z. (1995) *J. Chromatogr., A 718*, 59−66.
45. Cole, J. L. (1996) *Biochemistry 35*, 15601−15610.
46. Goto, Y., and Fink, A. L. (1989) *Biochemistry 28*, 945−952.
47. Rajah, R., Bhala, A., Lorraine, K., Nunn, S., Solberg, P., and Cohen, P. (1995) *Prog. Growth Res. 6*, 273−284.
48. Malm, J., Hellman, J., Hogg, P., and Lilja, H. (2000) *Prostate 45*, 132−139.
49. Okabe, E., Kajihara, J., Usami, Y., and Hirano, K. (1999) *FEBS Lett. 447*, 87−90.
50. Hedstrom, L., Perona, J. J., and Rutter, W. J. (1994) *Biochemistry 33*, 8757−8763.

51. Kerr, M. A., Walsh, K. A., and Neurath, H. (1975) *Biochemistry 14*, 5088−5094.

APPENDIX: THERMODYNAMIC INTERPRETATION OF THE ACTIVATION BY CONCENTRATED SALTS

It is known that salts at high concentrations (~1 M) are preferentially excluded from the surface of proteins in aqueous solution (*1*). The preferential exclusion follows the Hofmeister series. Preferential exclusion means that, at dialysis equilibrium, the binding stoichiometry, ν_L, is found to be negative. This means that the ligand (salt) has a lower affinity than water for the protein surface. Very weak ligands, such as concentrated salts, interact in a general nonspecific manner over the entire surface of the protein.

The thermodynamic meaning of binding is $\nu_L \equiv [\partial(m_L)/\partial(m_p)]_{\mu_L}$ [moles of ligand per mole of protein at constant chemical potential of ligand, i.e., at chemical (dialysis) equilibrium].

The measured binding, ν_L, is a measure of the mutual perturbations of the chemical potentials of the ligand and protein by each other:

$$\nu_L = -[\partial(\mu_p)/\partial(m_L)]_{m_p}/[\partial(\mu_L)/\partial(m_L)]_{m_p} \quad (1)$$

and

$$[\partial(\mu_p)/\partial(m_L)]_{m_p} = [\partial(\mu_L)/\partial(m_L)]_{m_L} \quad (2)$$

where μ is chemical potential [$\mu = \mu^\circ + RT(\ln m + \ln \gamma)$, where m is the concentration in molal units and γ is the activity coefficient].

Integration gives

$$\int_o^{m_L}[\partial(\mu_p)/\partial(m_L)]_{m_p} = dm_L = \Delta\mu_{p,tr} = \Delta G_b^o \quad (3)$$

where $\Delta\mu_{p,tr}$ is the free energy of transferring the protein from water to an aqueous solution of ligand of the given concentration (m_L), i.e., 1.3 M Na_2SO_4. This is the definition of the free energy of binding, ΔG_b^o.

Now if the measured binding, ν_L, is negative, $[\partial(\mu_p)/\partial(m_L)]_{m_p}$ is positive (eq 1) and ΔG_b^o is positive (eq 3). A positive free energy change is unfavorable, and the system will tend toward a more favorable state. Since weak ligands such as concentrated salts interact over the entire surface of the protein, one way to reduce the unfavorable interaction is to reduce the protein surface by a conformational change to a more compact structure (lower surface-to-volume ratio). This is shown schematically.

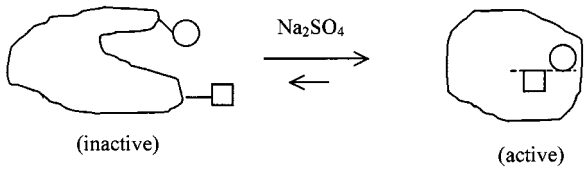

Part of the original surface vanishes into the "inside" of the protein; the molecule becomes more symmetrical, and groups exposed to solvent in state I and, hence, freely rotating, are drawn into the asymmetric environment of the protein interior in state II.

This simple mechanism of activation by a general thermodynamic effect can explain the observed salt effect. The enzyme must be capable of existing in two states in equilibrium, state I (inactive) and state II (active). The salt only displaces the equilibrium toward state II. This can account for the following observations. (1) The active form elutes more slowly from a size filtration column (more compact). (2) Some groups (Trp and Tyr) that are freely rotating on the surface in the inactive state become optically active, as they are drawn into the asymmetric environment of the protein interior.

This proposed mechanism of activation has the unusual features that the activator (salt) acts by not coming into contact with the enzyme (it is preferentially excluded), and that the driving force is repulsive (positive free energy of binding). For a detailed discussion of the theory, see ref *2* and references therein.

REFERENCES

1. Arakawa, T., and Timasheff, S. N. (1982) *Biochemistry 24*, 6545−6552.
2. Timasheff, S. N. (1998) *Adv. Protein Chem. 51*, 355−432.

BI010364J